

Vibrational Spectral Diffusion and Hydrogen Bond Dynamics in Heavy Water from First Principles

Bhabani S. Mallik, A. Semparithi,[†] and Amalendu Chandra*

Department of Chemistry, Indian Institute of Technology, Kanpur 208016, India

Received: February 17, 2008

We present a first-principles theoretical study of vibrational spectral diffusion and hydrogen bond dynamics in heavy water without using any empirical model potentials. The calculations are based on ab initio molecular dynamics simulations for trajectory generation and a time series analysis using the wavelet method for frequency calculations. It is found that, in deuterated water, although a one-to-one relation does not exist between the instantaneous frequency of an OD bond and the distance of its associated hydrogen bond, such a relation does hold on average. The dynamics of spectral diffusion is investigated by means of frequency–time correlation and spectral hole dynamics calculations. Both of these functions are found to have a short-time decay with a time scale of ~ 100 fs corresponding to dynamics of intact hydrogen bonds and a slower long-time decay with a time constant of ~ 2 ps corresponding to lifetimes of hydrogen bonds. The connection of the slower time scale to the dynamics of local structural relaxation is also discussed. The dynamics of hydrogen bond making is shown to have a rather fast time scale of ~ 100 fs; hence, it can also contribute to the short-time dynamics of spectral diffusion. A damped oscillation is also found at around 150–200 fs, which is shown to have come from underdamped intermolecular vibrations of a hydrogen-bonded water pair. Such assignments are confirmed by independent calculations of power spectra of intermolecular motion and hydrogen bond kinetics using the population correlation function formalism. The details of the time constants of frequency correlations and spectral shifts are found to depend on the frequencies of chosen OD bonds and are analyzed in terms of the dynamics of hydrogen bonds of varying strengths and also of free non-hydrogen-bonded OD groups.

1. Introduction

Studies of vibrational spectral diffusion within the stretch band of normal or deuterated water using ultrafast time-resolved infrared spectroscopy have provided a very powerful experimental means of investigating water dynamics at the molecular level.^{1–3} The vibrational frequencies of a water molecule are sensitive to its local solvation environment, and as the surrounding environment fluctuates due to molecular motion, the vibrational frequencies also fluctuate. The time dependence of these frequency fluctuations, known as vibrational spectral diffusion, captures the dynamics of the liquid at the molecular level such as the temporal evolution of hydrogen bonds in water. Many of the vibrational spectral diffusion experiments on normal or heavy water have employed nonlinear infrared pump–probe techniques such as transient hole-burning experiments, where a narrow band pump laser selectively excites a subset of OH or OD stretch modes from an inhomogeneous distribution of their frequencies, that is, a hole is created at the instant of laser excitation. When the system is subsequently probed by recording its transient absorption spectra at later times, the temporal evolution of the hole due to molecular motion and associated change in the average spectral frequency are observed. Although the analysis of these experiments is complicated by the presence of a number of other processes that also occur on similar time scales, mathematical models have been developed to extract the ground-state contribution to the pump–probe signal and also the time correlation function of fluctuating frequencies. Earlier

studies involving such transient hole-burning experiments on liquid water reported a time scale of 0.5–1.0 ps at room temperature.^{3–11} More recent experiments involving more sophisticated techniques, such as vibrational echos and two-dimensional infrared methods, which provide a better time resolution of spectral diffusion, have also revealed a shorter time scale of ~ 100 fs in addition to a longer time scale of about 1–2 ps.^{12–21}

On the theoretical side, all of the existing calculations of vibrational spectral diffusion are based on empirical potential models of liquid water. A majority of these studies consider a solute water immersed in a bath of classical water characterized by one of the existing potential models. The vibrational frequencies of the solute water are calculated by treating its nuclear motion quantum mechanically in the potential field of the surrounding classical water.^{22–28} There are also approaches that empirically relate the vibrational frequencies of the solute to instantaneous geometric configurations of the solvent.^{28–31} Very recently, Skinner and co-workers^{32–35} calculated the solute vibrational frequencies by first finding an empirical relationship between the frequency and electric field from a set of ab initio calculations of small solute–solvent clusters. Although these studies have provided important insight into various delicate issues of spectral diffusion, the spectral shifts as well as their dynamics can depend significantly on the details of the model potentials employed in the calculations. For example, the average OH frequency shift induced by the liquid water was calculated to be 212 cm^{-1} in ref 26, whereas only about half of that value was found in ref 27, the only difference between the two calculations being the use of different models for water intra- and intermolecular potentials. In addition to the average

* To whom correspondence should be addressed.

[†] Present address: Institut Charles Gerhardt (CTMM), CC 1501, Université Montpellier II-CNRS, 34095 Montpellier, Cedex 05, France.

frequency shifts, the width and height of the frequency distribution have also been found to differ from one model to the other.³⁴ Considerable variation in the dynamics of spectral diffusion has also been found for various water models,^{32–34} consistent with the previously known variability in other dynamical properties, like diffusion and orientational relaxation, calculated for different potential models of liquid water.^{36,37} For example, polarizable fluctuating charge models³⁸ of water predicted the longer-time slower decay of frequency correlations reasonably well but failed to reproduce the oscillations in the short-time dynamics, whereas nonpolarizable SPC/E³⁹ or TIP4P models,⁴⁰ although they could reproduce the short-time oscillations, predicted a significantly faster dynamics for the long-time part when compared with the corresponding experimental results.^{12–15,20,34} Hence, by changing the set of empirical water potentials, a significant variation in the frequency results can occur. Thus, it is desirable to calculate these equilibrium and dynamical aspects of vibrational spectral shifts from first principles without involving any empirical model potentials. Such a study is presented here for the first time. Although the focus of the present work is to present a finite-temperature *ab initio* computational method to calculate the dynamics of spectral diffusion and to aid in molecular-level interpretation of the observed results for liquid water, the same method can also be applied to other systems as well at the level of first principles.

In the present work, we perform a first-principles theoretical study of the vibrational spectral diffusion and hydrogen bond dynamics in deuterated liquid water by employing the methods of *ab initio* molecular dynamics^{41,42} for trajectory generation and wavelet analysis^{43–45} for frequency calculation. In *ab initio* molecular dynamics simulations, the quantum many-body potentials and forces are obtained directly from on-the-fly quantum electronic structure calculations, and thus, no empirical pair potentials are used. First, we investigated the equilibrium aspects of frequency–structure correlations in heavy water, especially the relations between the fluctuating stretch frequencies of OD modes and associated hydrogen bonds, and then, the dynamics of spectral diffusion was investigated by means of frequency–time correlation and spectral hole dynamics calculations. The dynamical results are analyzed in terms of the motion of an intact hydrogen-bonded pair and lifetimes of free and hydrogen-bonded states of OD bonds. The details of the time constants of frequency correlations and spectral shifts are found to depend on the frequencies of chosen OD bonds and are analyzed in terms of the dynamics of hydrogen bonds of varying strengths and also of free non-hydrogen-bonded OD groups. A first-principles calculation of the kinetics of local structural relaxation of hydrogen bonds is also presented using the population time correlation function formalism, and possible relations of such local structural relaxation to the observed dynamics of spectral diffusion are discussed.

The organization of the rest of the paper is as follows. In section 2, we present the details of *ab initio* molecular dynamics simulations, and in section 3, we discuss the wavelet analysis for frequency calculations. The results of frequency–structure correlations are discussed in section 4, and those of spectral diffusion and hydrogen bond dynamics are presented in section 5. Our conclusions are briefly summarized in section 6.

2. *Ab Initio* Molecular Dynamics Simulations

The *ab initio* molecular dynamics simulations were carried out by employing the Car–Parrinello method⁴² and the CPMD code.⁴⁶ Our simulation system contained 32 D₂O molecules in a cubic box of length 9.865 Å. We note that the size of the

simulation box used in the present simulations corresponds to the experimental density of liquid water at 300 K. The box was periodically replicated in three dimensions, and the electronic structure of the extended system was represented by the Kohn–Sham (KS) formulation⁴⁷ of density functional theory within a plane wave basis. The core electrons were treated via the norm-conserving atomic pseudopotentials of Troullier–Martins,⁴⁸ and the plane wave expansion of the KS orbitals was truncated at a kinetic energy of 80 Ry. A fictitious mass of $\mu = 800$ au was assigned to the electronic degrees of freedom, and the coupled equations of motion describing the system dynamics were integrated by using a time step of 5 au. We used the BLYP⁴⁹ functional in the present simulations because it has been shown to provide a good description of hydrogen-bonded liquids such as water,^{50,51} methanol,⁵² and also ammonia.⁵³ The initial configuration of the water molecules was generated by carrying out a classical molecular dynamics simulation using the empirical multisite SPC/E³⁹ interaction potential. Then, we equilibrated the system through *ab initio* molecular dynamics for 10 ps in a canonical ensemble at 300 K, and thereafter, we continued the run in the microcanonical ensemble for another 50 ps for calculations of various equilibrium and dynamical quantities.

Although the experiments in vibrational spectral diffusion have been performed on dilute mixtures of HOD in liquid H₂O or D₂O,^{1–21} our present simulations have been carried out for neat D₂O to make our calculations computationally more efficient. We note that one necessarily needs to either make a very long run of a system of one HOD in water or consider a very large system with several HODs in water at low concentration in order to obtain statistically meaningful results, but both these are not viable options for *ab initio* molecular dynamics. Instead, in the spirit of previous work,^{33,34} we simulated a neat liquid and considered, for the purpose of frequency calculations, that every OD bond of the neat liquid was an independent local vibration of interest. Thus, we calculated two OD vibrations of each water in the simulation system, giving a total of 64 local OD vibrations at every time instant, instead of only one, which would have been the case if we had considered just one HOD dissolved in 31 waters. We expected that the effects of this presumption that every bond in the system is a local oscillator of interest would not significantly affect our calculated results of spectral diffusion because experimental complications of excited-state vibrational energy relaxation through intermolecular resonant channels are not present in our simulation system. Besides, as discussed in the next section, the instantaneous frequencies were calculated directly from the simulated time dependence of OD oscillations, and thus, any effects of intermode coupling on the vibration of an OD group were implicitly taken into account in our calculations. Also, the analysis of spectral diffusion in terms of normal modes is complicated by the fact that the frequency perturbations of such modes come from two donor hydrogen bonds as compared to only one when the analysis is made within local mode approximation. Finally, while the equilibrium distribution of solute vibrational frequencies depends on solute mass and solute–solvent interactions, the normalized dynamics of the spectral diffusion is primarily sensitive to the molecular dynamics of the solvent. Thus, our calculated normalized dynamics can be compared with that obtained for OH modes in liquid D₂O under experimental situations. We note, however, that the experimental results of spectral diffusion in liquid H₂O and D₂O are rather similar, especially for the slower long-time part of the dynamics,^{2,15,17,20} and thus, our calculated results can be used to understand the basic aspects of spectral diffusion

in either of the two isotopic liquids. Also, the present calculations, as described in the following two sections, are of very general nature and can be straightforwardly extended to investigate spectral diffusion and related properties in other systems of experimental and theoretical interest such as ionic solutions^{54–61} including those containing acids and bases,^{62–67} interfaces,^{68–70} confined water,^{71–75} peptides and polypeptides in aqueous medium,^{76–80} and also nonaqueous systems.^{81–83}

3. Frequency Calculations: Time Series Analysis

A quantitative calculation of the time-dependent vibrational frequencies of OD bonds can be carried out through the so-called time series analysis of ab initio molecular dynamics trajectories. There are primarily two such approaches available in the literature to calculate the time-dependent frequencies associated with classical trajectories. The method of Laskar^{84,85} divides an entire trajectory into a series of short disjoint time intervals and uses windowed Fourier transforms in each of the short time intervals to obtain the instantaneous frequencies. The method of Arevalo and Wiggins,⁴⁴ on the other hand, obtains the time-dependent frequencies through a continuous wavelet transform of the trajectories. In the present work, we have followed this latter approach because it adjusts the size of the time window automatically according to the frequency of oscillations and thus provides a better localization in time of the spectral information of a trajectory than the approach of windowed Fourier transforms. The basic idea of the wavelet analysis is to express a time-dependent function $f(t)$ in terms of basis functions which are constructed as translations and dilations of a mother wavelet ϕ ⁴⁴

$$\psi_{a,b}(t) = a^{-1/2} \psi\left(\frac{t-b}{a}\right) \quad (1)$$

where the mother wavelet has to have compact support for it to be useful, that is, it should decay to zero rapidly for $t \rightarrow \pm\infty$. The coefficients of this expansion are given by the wavelet transform of $f(t)$, which is defined as

$$L_{\psi}f(a, b) = a^{-1/2} \int_{-\infty}^{\infty} f(t) \bar{\psi}\left(\frac{t-b}{a}\right) dt \quad (2)$$

for $a > 0$ and b real. For the mother wavelet, we have used the Morlet-Grossman wavelet⁸⁶

$$\psi(t) = \frac{1}{\sigma\sqrt{2\pi}} e^{2\pi i \lambda t} e^{-t^2/2\sigma^2} \quad (3)$$

with $\lambda = 1$ and $\sigma = 2$. The inverse of the scale factor a is proportional to the frequency, and thus, the wavelet transform of eq 2 at each b gives the frequency content of $f(t)$ over a time window about b . The width of the time window depends on a ; it automatically narrows for small a (high frequency) and widens for large a (low frequency). Since we are interested in the OD stretch frequencies, the time-dependent function $f(t)$ for a given OD bond is constructed to be a complex function with its real and imaginary parts corresponding to the instantaneous OD distance and the corresponding momentum along the OD bond. The value of the instantaneous stretch frequency at a given time $t = b$ is then determined from the scale a that maximizes the modulus of the corresponding wavelet transform at b , and the process is repeated for the entire 50 ps trajectory and for all of the 64 OD bonds which are there in the present simulation system.

4. Frequency–Structure Correlations: Equilibrium Aspects

Since the interpretation of the time-dependent vibrational spectral shifts is based on the key idea that the OD frequency

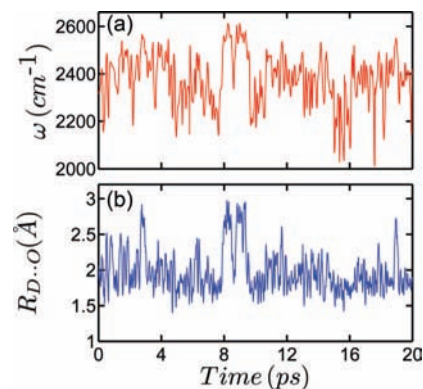


Figure 1. The fluctuating (a) frequency of a chosen OD bond and (b) distance of the D atom of this bond from its nearest oxygen of a neighboring molecule along the simulation trajectory.

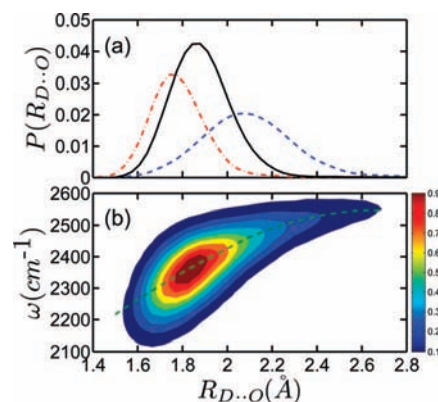


Figure 2. (a) The distribution of the D···O distance for fixed values of the OD frequency. The black solid, red dashed–dotted, and blue dashed curves are for OD frequencies $\Delta\omega = 0 \pm 5$, -100 ± 5 , and 100 ± 5 cm^{-1} , respectively, where $\Delta\omega$ represents the deviation from the average frequency. (b) Joint probability distribution of the OD frequency and D···O distance. The contour levels of different fractions of the maximum value are shown in different color codes.

is strongly correlated with the length of the hydrogen bond between the D atom and the nearest oxygen of a neighboring water, it is important to critically analyze from first principles the presence of any such frequency–structure correlations in the liquid phase of normal or heavy water. In Figure 1a, we have shown the time-dependent frequencies of a given OD bond as found from the wavelet method of time series analysis. In order to investigate the effects of nearest water on these fluctuating frequencies, in Figure 1b, we have shown the instantaneous distance of the nearest oxygen atom from the D atom of the OD mode. A correlation between the two fluctuating quantities is evident. In particular, when the D···O distance is large, for example, in the segment of 7.8–9.6 ps, the frequency is also found to be significantly higher than its average value.

The results shown above are for a particular OD bond. We now make a more detailed analysis of the relation between the frequency of an OD bond and the intermolecular D···O distance by averaging over all of the OD groups. In Figure 2a, we have shown the distribution of D···O distances for three fixed values of the OD frequency (within ± 5 cm^{-1}). For this figure, and also for Figures 5 and 6 shown later, we have used the MATLAB package to smooth the raw simulation data using the loess method with a span of about 5–15%.⁸⁷ It is seen that as the frequency increases, the corresponding distribution of D···O distances is also shifted toward its larger values. However, the distributions are fairly wide with significant overlaps, which means a single instantaneous frequency cannot

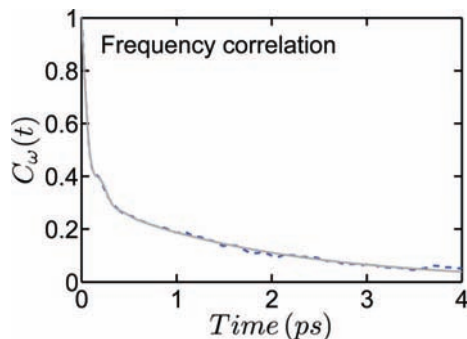


Figure 3. The time correlation function of OD fluctuating frequencies averaged over all of the molecules of the system. The blue dashed and solid grey curves correspond to the simulation data and fit by a function as given by eq 5, respectively.

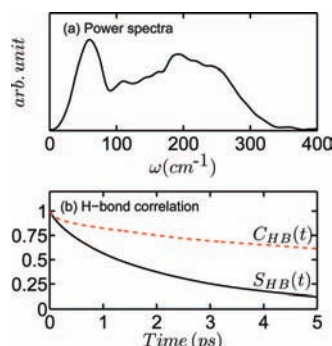


Figure 4. (a) The frequency dependence of the power spectra of O...O relative velocities of an initially hydrogen-bonded pair. (b) The time dependence of the continuous (black solid) and intermittent (red dashed) hydrogen bond time correlation functions.

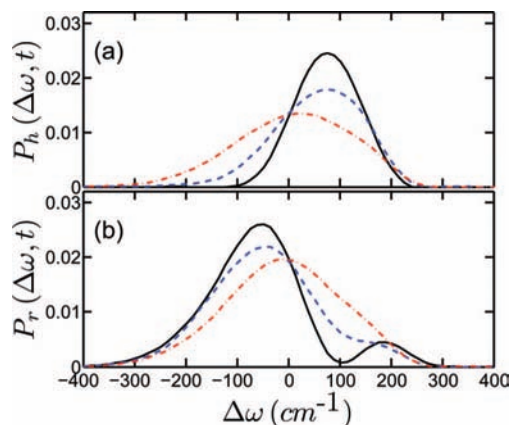


Figure 5. The time variation of the distribution of (a) hole and (b) remaining modes after excitation in the blue at time $t = 0$. The black solid, blue dashed, and red dashed-dotted curves are for times of 12 fs, 60 fs, and 1.5 ps, respectively.

be assigned to a given D...O distance. This is more clearly shown in Figure 2b through the contour plots of the conditional probability of observing a particular frequency for a given D...O distance. Clearly, there is substantial dispersion in the probability distribution which rules out the possibility of assigning a single instantaneous frequency to a given D...O distance. On average, however, the frequency is seen to be a monotonic function of the D...O distance, which means that a frequency-structure correlation is indeed present on average where the frequency of an OD bond decreases with the decrease of the associated D...O hydrogen bond distance. Although similar banana-shaped frequency-distance probability distributions were found earlier through empirical potential-based

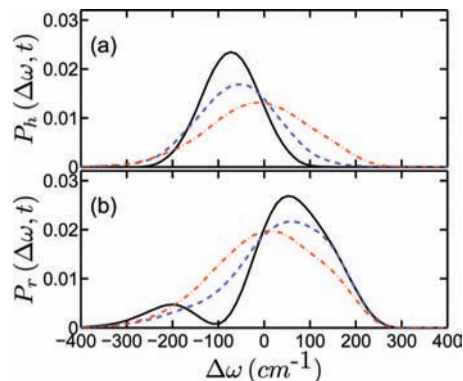


Figure 6. The time variation of the distribution of (a) hole and (b) remaining modes after excitation in the red at time $t = 0$. The black solid, blue dashed, and red dashed-dotted curves are for times of 12 fs, 60 fs, and 1.5 ps, respectively.

studies,^{24,26} a first-principles calculation of such a conditional probability distribution is presented here for the first time.

The distribution of all of the frequencies is found to be rather broad with a full width at half-maximum (fwhm) of 290 cm^{-1} and an average frequency ($\bar{\omega}$) of 2380 cm^{-1} (figure not shown). A separate simulation of gas-phase D₂O yields a frequency of 2560 cm^{-1} for the OD bonds; thus, the present calculations yield a Stokes shift of 180 cm^{-1} , which is to be compared with the experimental value of about 220 cm^{-1} for the OD stretch in liquid water.^{55,88} Apart from the frequency distribution, we also calculated the infrared (IR) spectra of the present system from dipole correlations within the high-temperature/harmonic approximation,⁸⁹ and the fwhm of the IR stretch band was found to be about 240 cm^{-1} (figure not shown), which is somewhat smaller than the width of the frequency distribution. However, we note that the IR band is expected to be somewhat narrower than the frequency distribution due to motional narrowing effects.^{26,90} Finally, we note that our calculated average stretch frequency of 2380 cm^{-1} is somewhat red-shifted compared to the corresponding experimental value of about 2500 cm^{-1} , which is likely due to the systematic errors introduced by the density functional, electronic fictitious mass, and finite basis set cutoff that are used in the electronic structure calculations^{91,92} and also may due to finite size of the simulation system. In principle, we could have accounted for these systematic errors by using a constant scaling factor, as was done in some of the earlier work.^{32,35} However, the primary focus of the present work is on the dynamics of spectral diffusion, and since the normalized dynamics remains unaltered by such scaling factors, we have preferred not to use any scaling factor in the present calculations to bring the calculated frequencies closer to experiments.

5. Spectral Diffusion and Hydrogen Bond Dynamics

5.1. Frequency-Time Correlation Function. The central dynamical object of interest in the context of vibrational spectral diffusion is the frequency-time correlation function defined by

$$C_{\omega}(t) = \langle \delta\omega(t)\delta\omega(0) \rangle / \langle \delta\omega(0)^2 \rangle \quad (4)$$

where $\delta\omega(t)$ is the fluctuation from the average frequency at time t . The average of eq 4 is over the initial time and over all of the OD groups of the system. The results of the frequency-time correlation are shown in Figure 3. A fast decay and an oscillation at around 200 fs are found in the short-time part of the dynamics, and this is then followed by a slower monotonic decay extending to a few ps. A biexponential fit to the entire

TABLE 1: Values of Various Time Constants (ps), Frequency (cm^{-1}), and Weights of Frequency–Time Correlation and Time-Dependent Frequency Shifts of Hole and Remaining Modes for Blue and Red Excitations

quantity	excitation	τ_0	τ_1	τ_2	ω_s	a_0	a_1
$C_\omega(t)$		0.10	0.12	2.0	136.1	0.19	0.50
$\Delta\bar{\omega}_h(t)$	blue	0.11	0.12	1.50	90.2	0.20	0.50
$\Delta\bar{\omega}_l(t)$	blue	0.13	0.13	3.60	112.6	0.17	0.54
$\Delta\bar{\omega}_h(t)$	red	0.18	0.13	3.10	111.5	0.10	0.57
$\Delta\bar{\omega}_l(t)$	red	0.16	0.11	1.4	92.0	0.15	0.50

decay yields two time scales of 100 fs and 1.85 ps with weights of 0.68 and 0.32, respectively. However, this biexponential fit does not reproduce the oscillation or bump that is found at around 200 fs, and thus, a fit including a damped oscillatory function is expected to reproduce better the simulation results. Indeed, a much better representation of the frequency correlation is found by using the fitting function²⁶

$$f(t) = a_0 \cos \omega_s t e^{-t/\tau_0} + a_1 e^{-t/\tau_1} + (1 - a_0 - a_1) e^{-t/\tau_2} \quad (5)$$

with the following values of the frequency and relaxation times: $\omega_s = 136.1 \text{ cm}^{-1}$, $\tau_0 \approx \tau_1 \approx 100 \text{ fs}$ and $\tau_2 \approx 2.0 \text{ ps}$. The details of the fitting parameters including the weights are included in Table 1. The oscillation in the short time is likely due to the underdamped motion of intact hydrogen-bonded $\text{O}\cdots\text{O}$ pairs. To confirm the origin of this oscillation, we have done a separate calculation of the power spectra of the relative velocity of an initially hydrogen-bonded $\text{O}\cdots\text{O}$ pair, which is shown in Figure 4a. Enhanced intensities are clearly visible at around 60 and 180 cm^{-1} in the power spectra arising from intermolecular bending and stretching vibrations of the hydrogen-bonded water pair. We note that these intermolecular vibrational frequencies agree well with the corresponding experimental values of 60 and 170 cm^{-1} for liquid D_2O .¹² Thus, the oscillations of the first term of eq 5 can be attributed to the fast intermolecular vibrations of intact hydrogen-bonded pairs. The exponential time constants of both the first and second terms are very similar, and they likely correspond to the short-time relaxation of the intact hydrogen bonds such as changes in the hydrogen bond length and angle that modulate the OD frequencies.

In an attempt to understand the origin of the slower relaxation component of the frequency–time correlation, we have calculated the dynamics of the breaking and making of hydrogen bonds in the system by using the so-called population correlation function approach. In this approach, we define two hydrogen bond population variables, $h(t)$ and $H(t)$, where $h(t)$ is unity when a particular water–water pair is hydrogen bonded at time t according to an adopted definition and zero otherwise and $H(t) = 1$ if the water–water pair remains continuously hydrogen bonded from $t = 0$ to time t , and it is zero otherwise. By constructing appropriate time correlations of these two population variables,^{92–98} we calculate two probability functions $S_{\text{HB}}(t)$ and $C_{\text{HB}}(t)$, where the first function describes the probability that an initially hydrogen-bonded water–water pair remains continuously bonded at all times up to t and the second function describes the probability that a water–water hydrogen bond is intact at time t , given that it was intact at time zero, independent of possible breaking in the interim time. While the integral of the continuous probability, τ_{HB} , can be interpreted as the average lifetime of a hydrogen bond, the time dependence of the intermittent probability describes the local structural relaxation of hydrogen bonds. After a hydrogen bond is broken, the water–water pair can remain as nearest neighbors for some time before either the bond is re-formed or the molecules diffuse

away from each other. We define $N_{\text{HB}}(t)$ as the time-dependent probability that a hydrogen bond is broken at time zero but the two molecules remain in the vicinity of each other, that is, as nearest neighbors, but are not hydrogen bonded at time t . Following previous work,^{92,94,96–98} we write a simple rate equation for the decay of $C_{\text{HB}}(t)$

$$\frac{-dC_{\text{HB}}(t)}{dt} = k_{\text{HB}} C_{\text{HB}}(t) - k'_{\text{HB}} N_{\text{HB}}(t) \quad (6)$$

where k_{HB} and k'_{HB} are the forward and backward rate constants and the inverse of k_{HB} can be interpreted as the average lifetime of a hydrogen bond. The existence of a hydrogen bond between the D (of OD) and the O of a neighboring water is found by using a simple geometric criterion that the $\text{D}\cdots\text{O}$ distance should be less than 2.45 \AA . On the other hand, two water molecules are taken to be nearest neighbors when their $\text{O}\cdots\text{O}$ distance is less than 3.4 \AA . Note that these distances correspond to the first minimum of the intermolecular $\text{O}\cdots\text{O}$ and $\text{D}\cdots\text{O}$ radial distribution functions (results not shown here). The results of the continuous and intermittent correlation functions are shown in Figure 4b. Integration of $S_{\text{HB}}(t)$ yields a value of 2.3 ps for τ_{HB} . We also applied a least-squares fit of the simulation results of $C_{\text{HB}}(t)$ and $N_{\text{HB}}(t)$ to eq 6 in the short-time region of $0 < t < 4 \text{ ps}$ to obtain the rate constants for the short-time part of the relaxation and in the longer time region of $4 < t < 12 \text{ ps}$ to calculate these quantities for the slower, long-time part of the relaxation. The inverses of the corresponding forward rate constants, which correspond to the average hydrogen bond lifetimes, are denoted as $1/k_{\text{HB};\text{short}}$ and $1/k_{\text{HB};\text{long}}$, and their values are found to be 2.0 and 13.0 ps, respectively. We note that the values of $1/k_{\text{HB};\text{short}}$ are similar to τ_{HB} obtained from the route of continuous correlation functions, which is expected because both $S_{\text{HB}}(t)$ and the short-time part of the reactive flux capture the hydrogen bond breaking dynamics due to librational, rotational, and short-time translational motion, and henceforth, this time constant of $\sim 2 \text{ ps}$ will be referred to as the hydrogen bond lifetime. A separate calculation of the residence dynamics of water molecules by following the method of refs 59 and 60 reveals that the longer time scale of $1/k_{\text{HB};\text{long}}$ actually corresponds to the residence time of a water molecule in the hydration shell of a tagged water to which it was hydrogen bonded at time $t = 0$. Thus, this longer time scale actually corresponds to escape dynamics or slow diffusion of a water molecule from its initial solvation shell.

From the similarity of the time scales, one can conclude that the slower relaxation time of the frequency correlation corresponds to lifetimes of hydrogen bonds. It would be instructive to investigate the dynamical contribution of the hydrogen bond making events to the overall spectral dynamics. For this purpose, we used a similar population–time correlation function formulation to calculate the probability of an OD, which was non-hydrogen-bonded (or free) at time $t = 0$, to remain continuously non-hydrogen-bonded up to time t . The integral of this time constant was found to be about 100 fs, which can be interpreted as the average time that an OD group remains free before it makes a hydrogen bond with a neighboring water molecule, and it is likely to contribute to the short-time part of the relaxation of the frequency correlation function. We note that our findings of a fast time scale of $\sim 100 \text{ fs}$ and a slower time scale of $\sim 2 \text{ ps}$ agree well with the results of recent time-resolved infrared spectroscopic experiments. For example, the long-time decay of the frequency correlation was reported to be 1.8 and 2 ps in refs 2 and 5, respectively, for the HOD/ H_2O system. In ref 15, the slower time scale was found to be 1.4 ps for HOD

in D₂O. We note in this context that earlier calculations using nonpolarizable water models predicted a time scale of 0.5 ps for TIP4P and 0.9 ps for SPC/E models^{24,32} for the long-time dynamics, which are shorter than the experimental value. The polarizable SPC-FQ model was found to give a time scale of 1.5 ps,³³ but it failed to reproduce the short-time oscillations found in experiments. To the best of our knowledge, none of the existing empirical models could quantitatively reproduce both the short-time oscillation and the slower long-time relaxation. The present first-principles study, on the contrary, is found to describe the dynamics of spectral diffusion quite well in both short-time and long-time regions.

It may be noted that the time dependence of the intermittent hydrogen bond correlation captures the dynamics of local structural relaxation, and the average decay time of this function is ~ 10 ps, which is significantly longer than the observed slower component of the dynamics of frequency correlation. Clearly, the slower time scale of spectral diffusion correlates better with the lifetime rather than the time scale of the much slower structural relaxation of hydrogen bonds. The structural relaxation, which definitely modulates the OD frequencies, can be viewed as a sequence of slow breaking and fast making processes of hydrogen bonds. Since the longer time scale in this composite relaxation process is that of the breaking of hydrogen bonds, it shows up as the slower component in the dynamics of spectral diffusion. In ref 15, the slower time scale in spectral diffusion was assigned to the time scale of switching of the partner through collective reorganization. Since the lifetime of a non-hydrogen-bonded water is very small, as found in the present calculations and also in earlier experiments,¹³ a true hydrogen bond breaking, as opposed to rattling between hydrogen-bonded and non-hydrogen-bonded states through intermolecular vibration, would indeed involve a switching of the hydrogen bond partner. In other words, given the very short lifetime of non-hydrogen-bonded water, true breaking of a hydrogen bond would occur only when a new partner has been found; thus, the dynamics of true hydrogen bond breaking and switching of the hydrogen bond partner are expected to occur on similar time scales. It is interesting to note that the frequency correlation function does not show a component corresponding to the slow escape dynamics of water molecules from a given solvation shell of another water. When a tagged D₂O molecule leaves its original first hydration shell centered on a D₂O, it simply enters the hydration shell of another D₂O without any noticeable changes in the frequency fluctuations (results not shown). Consequently, the much slower escape dynamics of water molecules is not captured in the time correlation of frequency fluctuations in pure water. However, the dynamics of such escape processes can give rise to a slow component in the spectral diffusion if the escape events take water molecules to different chemical environments, such as from ion solvation shells to bulk water in ionic solutions or from interfaces to bulk water for systems with liquid–liquid, liquid–vapor, or liquid–solid interfaces.

5.2. Hole Dynamics at Different Frequencies. In this section, we present a calculation of the dynamics of holes that are created by the removal of a band of OD frequencies in different frequency regions of the inhomogeneous equilibrium distribution. As noted in ref 26, the time evolution of these initially created nonequilibrium distributions is closely related to the time evolution of the pump–probe signals of time-dependent infrared spectroscopic experiments designed to investigate vibrational spectral diffusion in liquid water. Suppose at $t = 0$ that the laser pump pulse, which is assumed to have a

Gaussian frequency profile, burns a hole in the ground-state frequency distribution of the form

$$P_h(\omega, 0) = P_{eq}(\omega) e^{-(\omega - \omega_p)^2/2\sigma^2} \quad (7)$$

where ω_p is the pulse center frequency and $P_{eq}(\omega)$ denotes the equilibrium distribution of all of the OD frequencies in the system. Clearly, the initial distribution of the remaining OD frequencies $P_r(\omega, 0)$, that is, the ones remaining in the ground state in experimental situations, is equal to $P_{eq}(\omega) - P_h(\omega, 0)$. Following previous experimental and theoretical work,^{7–9,26} we use a Gaussian pulse of width (2σ) 140 cm⁻¹ and calculate the time evolution of the nonequilibrium distributions $P_r(\omega, t)$ and $P_h(\omega, t)$ from a large set of system trajectories reflecting the initial distributions $P_r(\omega, 0)$ and $P_h(\omega, 0)$, respectively. The average frequencies of the remaining and hole modes are then calculated from the following relation

$$\bar{\omega}_k(t) = \frac{1}{N_k} \int d\omega \omega P_k(\omega, t) \quad (8)$$

where $k = r$ for remaining modes and $k = h$ for the hole modes and $N_k = \int d\omega P_k(\omega, 0)$.

We have followed the dynamics of hole and remaining modes by creating holes in two different frequency regions: one centered in the red side at $\omega_p = \bar{\omega} - 100$ cm⁻¹ and the other centered in the blue side at $\omega_p = \bar{\omega} + 100$ cm⁻¹ where, as defined earlier, $\bar{\omega}$ is the average frequency of all of the OD groups in the system. We employed a Metropolis Monte Carlo-like algorithm⁹⁹ to effect the creation of a chosen hole, red or blue and at many different initial times, so as to satisfy the distribution of eq . We first show the time evolution of the hole and remaining distributions after the hole is created at $t = 0$. Since the hole is created instantly in our theoretical calculations, unlike in true experimental situations where creation of a hole of 140 cm⁻¹ width requires about 100 fs, its dynamics can be followed immediately after $t = 0$ in the present study. Of course, in experiments, one requires laser pulses of larger width to meaningfully measure the dynamics within the first 100 fs. The present theoretical results of the time evolution of hole and remaining distributions for blue excitation are shown in Figure 5, and the corresponding results for red excitation are shown in Figure 6. The frequency is expressed in terms of the shift ($\Delta\omega$) from its equilibrium value. When the hole is created in the blue, its distribution gradually shifts toward red until it becomes symmetric around the equilibrium frequency. The remaining distribution shifts toward blue with time, the hole in the blue region is gradually filled up, and finally, the distribution acquires a symmetric shape around $\bar{\omega}$, that is, around $\Delta\omega = 0$. Opposite shifts are found for the red excitation, as expected.

In Figure 7, we have shown the average frequencies of the hole modes ($\Delta\bar{\omega}_h$) for both blue and red excitations, and the corresponding results for the remaining modes ($\Delta\bar{\omega}_r$) are shown in Figure 8. Overall, the decay patterns of the average frequencies are found to be similar to that of the frequency time correlation function shown in Figure 3. There is a fast decay and an oscillation at short times followed by slower decay extending to a few ps. Interestingly, the oscillation is more pronounced in the dynamics of lower-frequency modes, such as the hole modes for red excitation and remaining modes for the blue excitation. Since the lower-frequency modes primarily involve strongly hydrogen-bonded OD modes, this again shows that the oscillations in the frequency evolution comes from underdamped intermolecular vibration of a hydrogen-bonded pair of molecules. Both bending and stretching modes of intermolecular vibrations can modulate the OD frequencies and

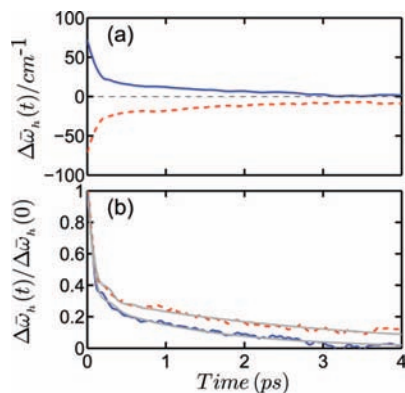


Figure 7. The time variation of the (a) average frequency shifts of the hole modes after excitations in the blue and in the red. The corresponding results after normalization by the initial frequency shifts are shown in (b). In both figures, the blue solid and red dashed curves corresponds to excitations in the blue and red, respectively. The grey solid curves in (b) represent the fits by a function of eq 5.

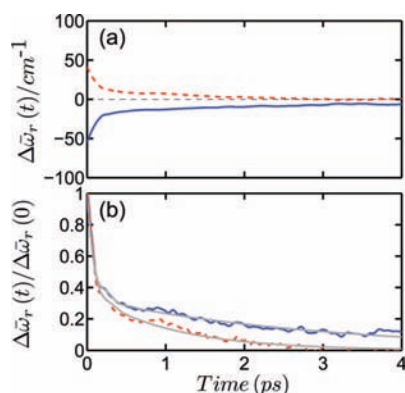


Figure 8. The time variation of the (a) average frequency shifts of the remaining modes after excitations in the blue and in the red. The corresponding results after normalization by the initial frequency shifts are shown in (b). In both figures, the blue solid and red dashed curves corresponds to excitations in the blue and red, respectively. The grey solid curves in (b) represent the fits by a function of eq 5.

hence contribute to the short-time oscillation of the hole dynamics. A fit of the type of eq 5 produces a fast time constant around 100–150 fs and a slower time constant around 1.5–3.5 ps; the details are included in Table 1. The shorter time scale corresponds to frequency modulation due to the dynamics of an intact hydrogen bond and also due to hydrogen bond making, especially for the high-frequency modes because many of them might have been non-hydrogen-bonded at the initial time. The longer time constant is again attributed to the lifetimes of hydrogen bonds. It is interesting to note that this slower relaxation has a longer time constant for the lower-frequency modes. For example, it is about 3 ps for the hole modes and 1.5 ps for the remaining modes in the case of excitation in the blue. This observation reaffirms the assignment of this slower time scale to hydrogen bond lifetimes. The lower frequency modes are characterized by stronger hydrogen bonds, on average, which have a longer lifetime.

6. Summary and Conclusions

We have presented a first-principles theoretical study of vibrational frequency–structure correlations and spectral diffusion in heavy water without employing any empirical model potentials. All D₂O molecules in the present study are considered on equal footing. They are allowed to interact with the full

many-body interaction potential obtained from quantum electronic structure calculations within the density functional formalism, and the whole system is propagated on the multi-dimensional electronic potential surface through the Car–Parrinello method.⁴² A time series analysis of the ab initio simulation trajectories using the wavelet transformation method reveals that although a one-to-one relation does not exist between the instantaneous frequency of an OD bond and the associated hydrogen bond distance, such a relation does hold, on average, where the frequency of an OD bond increases with an increase of the associated hydrogen bond distance. On the dynamical side of frequency fluctuations, it is found that the frequency–time correlation function has a short-time decay corresponding to the motion of intact hydrogen bonds and a long-time decay corresponding to the average lifetime of hydrogen bonds. The two time scales are around ~100 fs and ~2 ps, respectively. The possible role of local structural relaxation in the slower long-time dynamics of spectral diffusion is also discussed. The short-time dynamics of the frequency correlation can also have some contributions from hydrogen bond making events, which also occur on a time scale of ~100 fs. An oscillation is seen in the shorter time part of the dynamics, which arises from underdamped intermolecular vibrations of a hydrogen-bonded water pair. We also performed theoretical calculations of the time-dependent spectral shift by following the hole dynamics subsequent to excitations in the red and blue, and the results are analyzed in terms of the dynamics of intact and broken hydrogen bonds and also in terms of hydrogen bond lifetimes. The connections of the present first-principles results to recent time-dependent infrared spectroscopic experiments are also discussed.

The present study is based on a time-dependent frequency analysis of all of the OD bonds of a neat D₂O liquid from first-principles dynamical simulations. This choice of the system, where each OD mode is considered to be a local vibration of interest, greatly enhances the computational efficiency of our calculations. Also, use of the time series analysis of true simulated trajectories ensures that the effects of any intermode coupling of OD vibrations are implicitly taken into account in the present frequency calculations. The degeneracy of the two OD modes of an isolated water molecule is generally broken in the liquid phase due to asymmetric solvation, and the resultant frequency nondegeneracy is expected to provide some local character to the OD vibrations. In fact, an analysis of the calculated frequencies of the two OD modes of a given water in the simulated liquid reveals that the two bonds can vibrate at very different frequencies at a given time instance depending on their instantaneous solvation environment (results not shown); sometimes the difference can be as large as 400 cm⁻¹ or even more when one OD is strongly hydrogen bonded and the other one is free. Clearly, the asymmetric solvation of the two OD groups in liquid water can significantly break their gas-phase vibrational degeneracy.

We would also like to address the issue of stability of the present results with respect to the density functional employed in ab initio molecular dynamics simulations. For this purpose, we carried out a similar wavelet analysis of ab initio simulation trajectories of liquid D₂O obtained by using the HCTH/120 functional^{65,66,100} and calculated the frequency distribution and spectral diffusion properties. The fwhm of the frequency distribution and the average OD stretch frequency for this functional are found to be 280 and 2377 cm⁻¹, respectively, and the frequency correlation function is found to decay with times scales of 110 fs and 1.9 ps (figures not shown), which

are very close to the BLYP results presented in the previous sections. Thus, for pure D₂O, these two functionals are found to produce very similar results for vibrational spectral diffusion. Another issue that we would like to comment upon is the purely distance-based definition of a hydrogen bond that we have employed in the present study. Our calculated hydrogen bond lifetime (~2 ps) is a bit longer than the results for some of the empirical potentials where, in addition to the distance criteria, an angular cutoff was also used in the hydrogen bond definition.^{94–98,101} In fact, inclusion of angular cutoffs of 30 and 45° reduces our calculated hydrogen bond lifetimes to 1.25 and 1.65 ps, respectively, which are not very different from the results of well-parametrized model potentials, such as SPC/E.¹⁰¹ However, the hydrogen bond lifetime calculated with only the D···O distance criterion is found to agree better with our calculated spectral diffusion time for the same system, which is not unexpected because the frequency of an OD bond is primarily modulated by the fluctuations in the D···O distance.

The normalized dynamics of spectral diffusion primarily depends on the molecular dynamics of the solvent, and experimentally, the dynamics of spectral diffusion in liquid H₂O and D₂O have been found to be not very different from each other.^{2,15,17,20} Thus, the results of the present work can be used to understand the basic aspects of vibrational spectral diffusion in either of the two isotopic liquids. It may be noted that, at the qualitative level, the present first-principles study confirms many of the earlier results of empirical simulation models, such as the presence of primarily two time scales and a small oscillation in the dynamics of spectral diffusion, frequency distributions of hydrogen-bonded and non-hydrogen-bonded water molecules, and a banana-shaped frequency–distance conditional probability distribution. Hence, the present study provides support for using these models for spectral diffusion studies at the qualitative level. At the quantitative level, of course, some important differences exist. For example, none of the existing empirical models have been able to capture both the short- and the long-time dynamics correctly. While the nonpolarizable models like SPC/E and TIP4P describe the short-time oscillation reasonably well, they predict a too fast relaxation for the long-time component.^{24,25,32,34} whereas polarizable models like SPC-FQ or TIP4P-FQ, while predicting the long-time dynamics fairly well, fail to describe the short-time oscillation.^{33,34} The present first-principles study, on the other hand, describes both the short- and the long-time dynamics quite well without involving any adjustable potential parameters. We also note that empirical models alone, whether polarizable or nonpolarizable, cannot produce the time-dependent fluctuating frequencies along a simulation trajectory. Another level of approximation, such as a perturbative approach²⁵ or a different approximate potential of the solute HOD,^{23,24} had to be employed to extract the frequency fluctuations. On the contrary, the present methodology allows calculations of fluctuating frequencies directly from real-time ab initio simulation trajectories, and hence, it can be easily extended to study spectral diffusion in other related systems from first principles without employing any empirical model potentials.

Acknowledgment. We gratefully acknowledge financial supports from Department of Science and Technology (DST), Department of Atomic Energy (DAE), and Council of Scientific and Industrial Research (CSIR), Government of India, and the Alexander von Humboldt Foundation. We are thankful to Prof. S. Keshavamurthy for enlightening discussions and help in the initial stage of the frequency calculations.

References and Notes

- (1) Nibbering, E. T. J.; Elsaesser, T. *Chem. Rev.* **2004**, *104*, 1887.
- (2) Asbury, J. B.; Steinel, T.; Stromberg, C.; Corcelli, S. A.; Lawrence, C. P.; Skinner, J. L.; Fayer, M. D. *J. Phys. Chem. A* **2004**, *108*, 1107.
- (3) Bakker, H. J.; Kropman, M. F.; Omta, A. W.; Woutersen, S. *Phys. Scr.* **2004**, *69*, C14.
- (4) Laenen, R.; Rauscher, C.; Laubereau, A. *Phys. Rev. Lett.* **1998**, *80*, 2622.
- (5) Laenen, R.; Simeonidis, K.; Laubereau, A. *J. Phys. Chem. B* **2002**, *106*, 408.
- (6) Woutersen, S.; Emmerichs, U.; Bakker, H. J. *Science* **1997**, *278*, 658.
- (7) Woutersen, S.; Bakker, H. J. *Phys. Rev. Lett.* **1999**, *83*, 2077.
- (8) Gale, G. M.; Gallot, G.; Hache, F.; Lascoux, N.; Bratos, S. *Phys. Rev. Lett.* **1999**, *82*, 1068.
- (9) Bratos, S.; Gale, G. M.; Gallot, G.; Hache, F.; Lascoux, N.; Leickman, J.-C. *Phys. Rev. E* **1999**, *61*, 5211.
- (10) Wang, Z.; Pakoulev, A.; Pang, Y.; Dlott, D. D. *Chem. Phys. Lett.* **2003**, *378*, 281.
- (11) Pakoulev, A.; Wang, Z.; Pang, Y.; Dlott, D. D. *Chem. Phys. Lett.* **2003**, *371*, 594.
- (12) Fecko, C. J.; Eaves, J. D.; Loparo, J. J.; Tokmakoff, A.; Geissler, P. L. *Science* **2003**, *301*, 1698.
- (13) Eaves, J. D.; Loparo, J. J.; Fecko, C. J.; Roberts, S. T.; Tokmakoff, A.; Geissler, P. L. *Proc. Natl. Acad. Sci. U.S.A.* **2005**, *102*, 13019.
- (14) Eaves, J. D.; Tokmakoff, A.; Geissler, P. L. *J. Phys. Chem. A* **2005**, *109*, 9424.
- (15) Fecko, C. J.; Loparo, J. J.; Roberts, S. T.; Tokmakoff, A. *J. Chem. Phys.* **2005**, *122*, 054506.
- (16) Roberts, S. T.; Loparo, J. J.; Tokmakoff, A. *J. Chem. Phys.* **2006**, *125*, 084502.
- (17) (a) Loparo, J. J.; Roberts, S. T.; Tokmakoff, A. *J. Chem. Phys.* **2006**, *125*, 194521. (b) Loparo, J. J.; Roberts, S. T.; Tokmakoff, A. *J. Chem. Phys.* **2006**, *125*, 194522.
- (18) Stenger, J.; Madsen, D.; Hamm, P.; Nibbering, E. T. J.; Elsaesser, T. *J. Phys. Chem. A* **2002**, *106*, 2341.
- (19) Cowan, M. L.; Bruner, B. D.; Huse, N.; Dwyer, J. R.; Chugh, B.; Nibbering, E. T. J.; Elsaesser, T.; Miller, R. J. D. *Nature* **2005**, *434*, 199.
- (20) Steinel, T.; Asbury, J. B.; Corcelli, S. A.; Lawrence, C. P.; Skinner, J. L.; Fayer, M. D. *Chem. Phys. Lett.* **2004**, *386*, 295.
- (21) Asbury, J. B.; Steinel, T.; Kwak, K.; Corcelli, S. A.; Lawrence, C. P.; Skinner, J. L.; Fayer, M. D. *J. Chem. Phys.* **2004**, *121*, 12431.
- (22) Lawrence, C. P.; Skinner, J. L. *Chem. Phys. Lett.* **2003**, *369*, 472.
- (23) Lawrence, C. P.; Skinner, J. L. *J. Chem. Phys.* **2003**, *117*, 8847.
- (24) Lawrence, C. P.; Skinner, J. L. *J. Chem. Phys.* **2003**, *118*, 264.
- (25) Rey, R.; Moller, K. B.; Hynes, J. T. *J. Phys. Chem. A* **2002**, *106*, 11993.
- (26) Moller, K. B.; Rey, R.; Hynes, J. T. *J. Phys. Chem. A* **2004**, *108*, 1275.
- (27) Ojamäe, L.; Hermansson, K.; Probst, M. *Chem. Phys. Lett.* **1992**, *191*, 500.
- (28) Diraison, M.; Guissani, Y.; Leickman, J. C.; Bratos, S. *Chem. Phys. Lett.* **1996**, *258*, 348.
- (29) Brudermann, J.; Meljer, M.; Buck, U.; Kazimirski, J. K.; Sadlej, J.; Buch, V. *J. Chem. Phys.* **1999**, *110*, 10649.
- (30) Sadlej, J.; Buch, V.; Kazimirski, J. K.; Buck, U. *J. Phys. Chem. A* **1999**, *103*, 4933.
- (31) Cho, M. *J. Chem. Phys.* **2003**, *118*, 3480.
- (32) Corcelli, S. A.; Lawrence, C. P.; Skinner, J. L. *J. Chem. Phys.* **2004**, *120*, 8107.
- (33) Corcelli, S. A.; Lawrence, C. P.; Asbury, J. B.; Steinel, T.; Fayer, M. D.; Skinner, J. L. *J. Chem. Phys.* **2004**, *121*, 8897.
- (34) Schmidt, J. R.; Roberts, S. T.; Loparo, J. J.; Tokmakoff, A.; Fayer, M. D.; Skinner, J. L. *Chem. Phys.* **2007**, *341*, 143.
- (35) Auer, B.; Kumar, R.; Schmidt, J. R.; Skinner, J. L. *Proc. Natl. Acad. Sci. U.S.A.* **2007**, *104*, 14215.
- (36) van der Spoel, D.; van Maaren, P. J.; Berendsen, H. J. C. *J. Chem. Phys.* **1998**, *108*, 10220.
- (37) Chandra, A.; Ichiye, T. *J. Chem. Phys.* **1999**, *111*, 2701.
- (38) Rick, S. W.; Stuart, S. J.; Berne, B. J. *J. Chem. Phys.* **1994**, *101*, 6141.
- (39) Berendsen, H. J. C.; Grigera, J. R.; Straatsma, T. P. *J. Phys. Chem.* **1987**, *91*, 6269.
- (40) Jorgensen, W. L.; Chandrasekhar, J.; Madura, J. D.; Impey, R. W.; Klein, M. L. *J. Chem. Phys.* **1983**, *79*, 926.
- (41) Marx, D.; Hutter, J. *Ab Initio Molecular Dynamics: Theory and Implementation in Modern Methods and Algorithms of Quantum Chemistry*; Grotendorst, J., Ed.; NIC: FZ Jülich, 2000; for downloads, see: www.theochem.ruhr-uni-bochum.de/go/prev.html.
- (42) Car, R.; Parrinello, M. *Phys. Rev. Lett.* **1985**, *55*, 2471.

- (43) Fuentes, M.; Guttorp, P.; Sampson, P. D. In *Statistical Methods for Spatio-Temporal Systems*; Finkenstädt, B., Held, L., Isham, V., Eds.; Chapman & Hall/CRC: Boca Raton, 2007; Chapter 3.
- (44) Vela-Arevalo, L. V.; Wiggins, S. *Int. J. Bifurcation Chaos Appl. Sci. Eng.* **2001**, *11*, 1359.
- (45) Semparithi, A.; Keshavamurthy, S. *Phys. Chem. Chem. Phys.* **2003**, *5*, 5051. See section IV for a calculation of time-dependent frequencies using the wavelet method.
- (46) Hutter, J.; Alavi, A.; Deutsch, T.; Bernasconi, M.; Goedecker, S.; Marx, D.; Tuckerman, M.; Parrinello, M. *CPMD Program*; MPI für Festkörperforschung und IBM Zurich Research Laboratory.
- (47) Kohn, W.; Sham, L. J. *Phys. Rev. A* **1965**, *140*, 1133.
- (48) Troullier, N.; Martins, J. L. *Phys. Rev. B* **1991**, *43*, 1993.
- (49) (a) Becke, A. D. *Phys. Rev. A* **1988**, *38*, 3098. (b) Lee, C.; Yang, W.; Parr, R. G. *Phys. Rev. B* **1988**, *37*, 785.
- (50) Laasonen, K.; Sprik, M.; Parrinello, M.; Car, R. *J. Chem. Phys.* **1993**, *99*, 9080.
- (51) Sprik, M.; Hutter, J.; Parrinello, M. *J. Chem. Phys.* **1995**, *105*, 1142.
- (52) Tsuchida, E.; Kanada, Y.; Tsukada, M. *Chem. Phys. Lett.* **1999**, *311*, 236.
- (53) Boese, D.; Chandra, A.; Martin, J. M. L.; Marx, D. *J. Chem. Phys.* **2003**, *119*, 5965.
- (54) (a) Kropman, M. F.; Bakker, H. J. *Science* **2001**, *291*, 2118. (b) Kropman, M. F.; Bakker, H. J. *J. Chem. Phys.* **2001**, *115*, 8942.
- (55) Park, S.; Fayer, M. D. *Proc. Natl. Acad. Sci. U.S.A.* **2007**, *104*, 16731.
- (56) Nigro, B.; Re, S.; Laage, D.; Rey, R.; Hynes, J. T. *J. Phys. Chem. A* **2006**, *110*, 11237.
- (57) Laage, D.; Hynes, J. T. *Proc. Natl. Acad. Sci. (U.S.A.)* **2007**, *104*, 11167.
- (58) Li, S.; Schmidt, J. R.; Piryatinski, A.; Lawrence, C. P.; Skinner, J. L. *J. Phys. Chem. B* **2006**, *110*, 18933.
- (59) Chowdhuri, S.; Chandra, A. *J. Phys. Chem. B* **2006**, *110*, 9674.
- (60) Mallik, B. S.; Chandra, A. *J. Chem. Phys.* **2006**, *125*, 234502.
- (61) (a) Raugei, S.; Klein, M. L. *J. Am. Chem. Soc.* **2001**, *123*, 9484. (b) Raugei, S.; Klein, M. L. *J. Chem. Phys.* **2002**, *116*, 196.
- (62) Woutersen, S.; Bakker, H. J. *Phys. Rev. Lett.* **2006**, *96*, 138305.
- (63) Nienhuys, H.-K.; Lock, A. J.; van Santen, R. A.; Bakker, H. J. *J. Chem. Phys.* **2002**, *117*, 8027.
- (64) Rini, M.; Magnes, B.-Z.; Pines, E.; Nibbering, E. T. J. *Science* **2003**, *301*, 349.
- (65) Tuckerman, M.; Chandra, A.; Marx, D. *Acc. Chem. Res.* **2006**, *39*, 151.
- (66) Chandra, A.; Tuckerman, M.; Marx, D. *Phys. Rev. Lett.* **2007**, *99*, 145901.
- (67) Dellago, C.; Hummer, G. *Phys. Rev. Lett.* **2006**, *97*, 245901.
- (68) Scatena, L. F.; Brown, M. G.; Richmond, G. L. *Science* **2001**, *292*, 908.
- (69) Shultz, M. J.; Baldelli, S.; Schnitzer, C.; Simonelli, D. *J. Phys. Chem. B* **2002**, *106*, 5313.
- (70) (a) Paul, S.; Chandra, A. *J. Chem. Phys.* **2005**, *123*, 174712. (b) Paul, S.; Chandra, A. *J. Chem. Theory Comput.* **2005**, *1*, 1221.
- (71) Gillijamse, J. J.; Lock, A. J.; Bakker, H. J. *Proc. Natl. Acad. Sci. U.S.A.* **2005**, *102*, 3202.
- (72) Tan, H.-S.; Piletic, I. R.; Riter, R. E.; Levinger, N. E.; Fayer, M. D. *Phys. Rev. Lett.* **2005**, *94*, 057405.
- (73) Vaitheewaran, S.; Yin, H.; Rasaiah, J. C.; Hummer, G. *Proc. Natl. Acad. Sci. U.S.A.* **2004**, *101*, 17002.
- (74) Lakatos, G.; Patey, G. N. *J. Chem. Phys.* **2007**, *126*, 024703.
- (75) Sahu, K.; Mondal, S. K.; Ghosh, S.; Bhattacharyya, K. *Bull. Chem. Soc. Jpn.* **2007**, *80*, 1033.
- (76) Hamm, P.; Lim, M.; DeGrado, W. F.; Hochstrasser, R. M. *Proc. Natl. Acad. Sci. U.S.A.* **1999**, *96*, 2036.
- (77) Scheurer, C.; Priyatinski, A.; Mukamel, S. *J. Am. Chem. Soc.* **2001**, *123*, 3114.
- (78) Mu, Y.; Stock, G. *J. Phys. Chem. B* **2002**, *106*, 5294.
- (79) Gorbunov, R. D.; Nguyen, P. H.; Kobus, M.; Stock, G. *J. Chem. Phys.* **2007**, *126*, 054509.
- (80) (a) Kwac, K.; Cho, M. *J. Chem. Phys.* **2003**, *119*, 2247. (b) Kwac, K.; Cho, M. *J. Chem. Phys.* **2003**, *119*, 2256.
- (81) Asbury, J. B.; Steinel, T.; Stromberg, C.; Gaffney, K. J.; Piletic, I. R.; Goun, A.; Fayer, M. D. *Phys. Rev. Lett.* **2003**, *91*, 237402.
- (82) Asbury, J. B.; Steinel, T.; Fayer, M. D. *J. Phys. Chem. B* **2004**, *108*, 6544.
- (83) Stenger, J.; Madsen, D.; Dreyer, J.; Nibbering, E. T. J.; Hamm, P.; Elsaesser, T. *J. Phys. Chem. A* **2001**, *105*, 2929.
- (84) Laskar, J.; Froeschle, C.; Celletti, A. *Physica D* **1992**, *56*, 253.
- (85) Laskar, J. *Physica D* **1993**, *67*, 257.
- (86) Carmona, R.; Hwang, W.; Torresani, B. *Practical Time-Frequency Analysis: Gabor and Wavelet Transforms with an Implementation*; Academic Press: New York, 1998.
- (87) Matlab, version-R2007a, The MathWorks, Inc., U.S.A. <http://www.mathworks.com>.
- (88) Bernath, P. *Phys. Chem. Chem. Phys.* **2002**, *4*, 1501.
- (89) Ramirez, R.; Lopez-Ciudad, T.; P Kumar, P.; Marx, D. *J. Chem. Phys.* **2004**, *121*, 3973.
- (90) Ojamäe, L.; Tegenfeldt, J.; Lindgren, J.; Hermansson, K. *Chem. Phys. Lett.* **1992**, *195*, 97.
- (91) Kuo, I.-F. W.; Tobias, D. J. *J. Phys. Chem. A* **2002**, *106*, 10969.
- (92) Lee, H.-S.; Tuckerman, M. E. *J. Chem. Phys.* **2007**, *126*, 164501-1.
- (93) Rapaport, D. *Mol. Phys.* **1983**, *50*, 1151.
- (94) Chandra, A. *Phys. Rev. Lett.* **2000**, *85*, 768.
- (95) Balasubramanian, S.; Pal, S.; Bagchi, B. *Phys. Rev. Lett.* **2002**, *89*, 115505.
- (96) (a) Luzar, A.; Chandler, D. *Phys. Rev. Lett.* **1996**, *76*, 928. (b) Luzar, A.; Chandler, D. *Nature (London)* **1996**, *379*, 53.
- (97) Xu, H.; Berne, B. J. *J. Phys. Chem. B* **2001**, *105*, 11929.
- (98) Xu, H.; Stern, H. A.; Berne, B. J. *J. Phys. Chem. B* **2002**, *106*, 2054.
- (99) Allen, M. P.; Tildesley, D. J. *Computer Simulation of Liquids*; Oxford: New York, 1987.
- (100) Boese, A. D.; Doltsinis, N. L.; Handy, N. C.; Sprik, M. *J. Chem. Phys.* **2000**, *112*, 1670.
- (101) (a) Chandra, A. *J. Phys. Chem. B* **2003**, *107*, 3899. (b) Chowdhuri, S.; Chandra, A. *J. Phys. Chem. B* **2006**, *110*, 9674.

JP801405A